Evidence of Nitric Acid Uptake in Warm Cirrus Anvil Clouds during the NASA TC4 Campaign

Eric Scheuer, Jack E. Dibb

Institute for the Study of Earth, Oceans and Space, University of New Hampshire, Durham, NH

Cynthia Twohy

College of Oceanic and Atmospheric Sciences, Oregon State University, Corvallis, OR

David C. Rogers

National Center for Atmospheric Research, Research Aviation Facility, Broomfield, CO

Andrew J. Heymsfield, Aaron Bansemer

National Center for Atmospheric Research, Earth and Sun Systems Laboratory, Boulder, CO

corresponding author: Eric Scheuer, eric.scheuer@unh.edu, 603.862.2284

For submission to the special issue of JGR Atmospheres on NASA TC4

21 September 2009

Abstract.

Uptake of HNO_3 onto cirrus ice may play an important role in tropospheric NO_x cycling. Discrepancies between modeled and in situ measurements of gas-phase HNO_3 in the troposphere suggest that redistribution and removal mechanisms by cirrus ice have been poorly constrained. Limited in situ measurements have provided somewhat differing results and are not fully compatible with theory developed from laboratory studies. We present new airborne measurements of HNO_3 in cirrus clouds from anvil outflow made during the Tropical Composition, Cloud, and Climate Coupling Experiment (TC4). Upper tropospheric (>9km) measurements made during three flights while repeatedly traversing the same cloud region revealed depletions of gas-phase HNO_3 in regions characterized by higher ice water content and surface area. We hypothesize that adsorption of HNO_3 onto cirrus ice surfaces could explain this. Using measurements of cirrus ice surface area density and some assumptions about background mixing ratios of gas-phase HNO_3, we estimate molecular coverages of HNO_3 on cirrus ice surface in the tropical upper troposphere during the TC4 racetracks to be about 1×10^{13} molecules·cm^{-2}. This likely reflects an upper limit because potential dilution by recently convected, scavenged air is ignored. Also presented is an observation of considerably enhanced gas-phase HNO_3 at the base of a cirrus anvil suggesting vertical redistribution of HNO_3 by sedimenting cirrus particles and subsequent particle sublimation and HNO_3 evaporation. The impact of released HNO_3, however, appears to be restricted to a very thin layer just below the cloud.

1. Introduction

Gas-phase nitric acid, HNO_3, is a primary reservoir species of atmospheric nitrogen oxides ($NO_x = NO+NO_2$) [Neuman et al., 2001; Staudt et al., 2003] which play an important role in upper tropospheric ozone production [Jacob et al. 1996]. Early global chemistry models generally over predicted upper tropospheric (UT) HNO_3 by factors ranging from two to ten [Thakur et al., 1999] suggesting, in part, that removal mechanisms were poorly understood. Recent implementations of the GEOS-Chem and RAQMS models in Hudman et al. [2007] and Pierce et al. [2007] showed significant improvement, but still generally overestimate upper UT HNO_3 when compared to aircraft measurements. Lawrence and Crutzen [1998] suggested that efficient removal by adsorptive uptake onto cirrus cloud ice particles and subsequent gravitational sedimentation had the potential to significantly redistribute or remove HNO_3 in the UT explaining some of the discrepancies between measurements and models. Initial laboratory investigations into HNO_3 uptake onto ice surfaces found that this process is efficient, and appears to proceed until there is a high fractional surface coverage of available adsorption sites. However, details of the uptake have varied between experiments using ice particles and films, and may be less than ideal surrogates for crystals in cirrus clouds. Also, most of these experiments were performed using HNO_3 partial pressures greatly in excess of those likely in the UT requiring large and poorly constrained extrapolations to relevant vapor pressures [Abbat, 1997; Zondlo et al., 1997; Arora et al., 1999; Hudson et al., 1999; Hynes et al., 2002]. Tabazadeh et al. [1999] assessed the results of several lab studies and presented a Langmuir surface chemical model that assumed the isotherm was dissociative and concluded that uptake of HNO_3 onto cirrus may be nearly an order of magnitude less efficient than Lawrence and Crutzen [1998] assumed. Tabazadeh et al. [1999] also suggested that sublimation of cirrus crystals within several

63 kilometers below clouds would limit the extent of vertical redistribution of HNO_3 by this
64 process. A box model employed by Meier and Hendricks [2002] expanded on the assumptions in
65 Tabazadeh et al. [1999] for a much wider range of ambient conditions and sedimentation
66 efficiencies and suggested under some conditions that HNO_3 uptake on cirrus ice and
67 gravitational sedimentation could still be an efficient denitrification mechanism. Laboratory
68 studies by Ullerstam et al. [2005] were the first to be performed at HNO_3 partial pressures more
69 typical of the UT and confirmed some aspects of prior studies. HNO_3 uptake on ice surfaces in
70 these experiments was found to be positively correlated with overlying HNO_3 partial pressures at
71 low vapor pressures and available ice surface area, and negatively correlated with temperature.
72 However surface coverage was found to be far from a complete molecular monolayer at partial
73 pressures of HNO_3 typical of the UT, and uptake followed conventional non-dissociative
74 Langmuir isotherm. Ullerstam et al. [2005] also noted that conventional and non-dissociative
75 Langmuir treatments of HNO_3 uptake on ice predict similar behavior at high vapor pressures but
76 diverged markedly at low pressures.

77 The first in situ aircraft measurements to provide evidence for uptake of HNO_3 by cirrus
78 ice were reported by Weinheimer et al. [1998]. They measured the sum of condensed plus gas
79 phase NO_y through a forward facing inlet compared to a gas phase only rear facing inlet to infer
80 that up to 20% of NO_y was adsorbed onto ice in a mountain wave cloud over Colorado. Nitric
81 acid was assumed to be the only component of NO_y taken up by ice. Surface coverages on the
82 cirrus crystals were later estimated to be in the range of 1-4 x 10^{13} molecules·cm^{-2} for
83 measurements made near the tropopause at ~215 K [Hudson et al., 2002]. Several subsequent
84 aircraft studies have also used similar dual inlet equipped NO_y instruments to "observe" HNO_3
85 on ice crystals in the UT. Melinger et al. [1999] estimated coverages of 1 x 10^{13} molecules·cm^{-2}

in Arctic cirrus at ~196 K, much lower than estimates near 2 x 10^{14} molecules·cm^{-2} reported by Kondo et al. [2003] in Arctic clouds at temperatures ~210 K. Extensive measurements at mid-latitudes reported by Ziereis et al. [2004] indicate coverages in the range 1 - 10 x 10^{13} and 0.5 - 1.5 x10^{13} molecules·cm^{-2} at 214 K and 227 K, respectively. In both cases, the inferred vapor pressure of HNO_3 corresponding to the high end of the estimated molecular coverage range was a factor of four greater than estimates for the low end of the range. Direct measurements of condensed and gas phase HNO_3 in subtropical cirrus during the NASA CRYSTAL-FACE campaign are presented by Popp et al. [2004]. These data were also obtained with a similar dual inlet arrangement, but HNO_3 was quantified directly by chemical ionization mass spectrometry (CIMS) rather than inferred from NO_y measurements. Mean surface coverages of 6 x 10^{13} molecules·cm^{-2} at 198 K and about 2 x 10^{13} molecules·cm^{-2} for four 5 K bins from 200 K - 220 K were estimated. Popp et al. [2004] suggested that the samples at temperatures below 200 K were impacted by nitric acid trihydrate (NAT), thus not truly comparable to cirrus ice and point out that the rest of their observations indicate very weak, or no, dependence on temperature. Ullerstam et al. [2005] compared the results of these different field studies and suggested that overall the studies on thin ice films in flow tubes were qualitatively consistent and concluded that HNO_3 uptake in real clouds should generally increase at higher HNO_3 vapor pressures and at lower temperatures (though the Melinger et al. [1999] results do not fit this generalization with very low estimated surface coverages at cold temperatures). They also noted, however, that when a conventional non-dissociative Langmuir isotherm model fitted to their laboratory results was used to estimate surface coverages at the conditions of the various field studies, observed values were generally smaller than the estimates.

In this paper, we report the first field evidence for uptake of HNO_3 onto tropical cirrus crystals in the intertropical convergence zone (ITCZ) near Costa Rica using measurements of gas phase HNO_3, ice water content (IWC), and surface area density (SAD). These observations extend the temperature range of in situ studies nearly to 245 K and explore quite low HNO_3 vapor pressures. Simultaneous measurements of condensed phase HNO_3 are not available, adding uncertainty to our quantitative estimates of HNO_3 surface coverage on ice, but we suggest the estimates are still informative because they are based on observations in quite warm cirrus several kilometers below the tropopause.

2. Methods

2.1 TC4 Mission

NASA's Tropical Composition, Cloud and Climate Coupling (TC4) experiment in July and August, 2007 deployed the DC-8, ER-2 and WB-57 aircraft to Costa Rica to study deep convection in the ITCZ and its impact on the tropical tropopause layer (TTL) [Toon et al., this issue]. The primary role of the DC-8 was expected to be characterizing the chemical and microphysical properties of the troposphere to constrain the composition of air being entrained into the convection. However, during flights much of the convective outflow and resulting cirrus near Costa Rica during the campaign was close to the 13 km ceiling of the DC-8. As a result, roughly half of all DC-8 sampling time targeted the UT (9-13 km) and most of that time was in and near cirrus clouds. Here we report on observations of in situ HNO_3, IWC, and SAD during three flights that targeted cirrus shields from specific convective cores to examine the extent of depletion of gas phase HNO_3 by uptake on ice crystals in these clouds.

2.2 HNO_3 Measurements

Gas phase nitric acid was measured with the University of New Hampshire automated dual mist chamber/ion chromatograph system (MC/IC). In this system, ambient air is drawn into the aircraft at high velocity through a short (<1 meter), Silcosteel® (Restek, Inc., Bellefonte, PA) coated manifold at approximately 3 m^3 (volumetric) min^{-1}. Ambient air is sub-sampled at approximately 45-50 L min^{-1} (volumetric) by one of a pair of glass mist chambers mounted on the high flow manifold. The mist chamber inlets are rear facing with respect to the flow in the manifold which, based on stopping distance calculations from Hinds [1982], should effectively exclude particles greater than ~1 μm . This implies that any potential positive artifact arising from evaporation of the much larger ice crystals in the manifold is minimized. Discrete samples integrated for approximately 85 seconds are alternately collected by each mist chamber. While one mist chamber is sampling, the preceding sample collected in the other mist chamber is injected into an ion chromatograph where HNO_3 is detected as the NO_3^- ion. HNO_3 detection limits varied inversely with the mist chamber mass flow rate which decreases with altitude, but were typically better than 3 parts per trillion by volume (pptv). Overall measurement uncertainty of HNO_3 for values less than 25 pptv is believed to be 30-35%; about 20% for values between 25 and 100 pptv, and 15% for values above 100 pptv. Variants of this instrument have been flown on the DC-8 on more than 10 other campaigns (TRACE-A, PEM-WEST A and B, PEM-TROPICS A and B, SONEX, PAVE, TRACE-P, INTEX A and B, ARCTAS).

2.3 Ice Water Content Measurements

Ice water content (IWC) in cirrus cloud was measured using the National Center for Atmospheric Research (NCAR) counterflow virtual impactor (CVI) as described by Twohy et. al. [1997]. Ice crystals with aerodynamic diameters greater than about 5 microns are separated from interstitial air using dry nitrogen counter flow at the inlet tip of the forward facing inlet. A

153 tunable diode laser hygrometer is used to measure the water content after ice crystals are
154 evaporated within the inlet. Uncertainty in individual measurements is typically about 15%, but
155 varies with measurement magnitude and can be considerably higher at very low values. For
156 example, for IWC values near 0.5 $g \cdot m^3$, uncertainty is 11-13% and for IWC values of 0.005 $g \cdot m^3$
157 uncertainty is 15-24%.

158 2.4 Ice Surface Area Density Measurements

159 Particle size distributions (PSD) were measured by two-dimensional cloud and
160 precipitation imaging probes (CIP, PIP) covering the size range from about 50 to 3000 microns.
161 Projected areas given by the 2D images of the particles were measured, which, together with the
162 PSD's, gave distributions of particle cross-sectional area per unit volume. It was desirable to
163 average the 2D probe data over 5-sec intervals to ensure that sufficient numbers of particles 1
164 mm and above, normally present in low concentrations, were obtained. The 2D probe data have
165 been processed objectively to remove artifacts produced by shattering on the probes' leading
166 edges (see Field et al. [2003]). While difficult to constrain, individual SAD measurements are
167 believed to be +/- ~25%.

168 All data and analyses presented here are temporally merged where the IWC and SAD
169 observations are averaged over the integration time of each mist chamber sample. All original
170 data are available from the NASA Earth Science Project Office (ESPO) archive.

171 3. Results

172 We focus on three flights conducted on 31 July, 5 August, and 8 August, 2007. During
173 these flights, extended periods of time were spent flying in orbital "racetrack" patterns within
174 cirrus clouds (Figure 1). The purpose of the racetracks was to observe the evolution of cloud

175 microphysical characteristics as measured by a number of in situ sensors on the DC-8 and by
176 remote sensors deployed on the ER-2 which simultaneously conducted the same racetrack flight
177 patterns above the clouds (e.g., Jensen et al., 2009, Tian et al., this issue). The straight legs of
178 each oval were typically about 20 minutes long (~ 200 km) with the turns at each end making the
179 horizontal extent of each oval roughly 250 km. The tangent point of upwind turns were set up in
180 real time to be about 10 km downwind of the convective turret of a cirrus anvil identified by the
181 flight planning team at base from rapid-update GOES imagery. The 31 July flight targeted cirrus
182 clouds streaming to the south east from a convective complex that was visible from the
183 operations base at Juan Santamaria airport near San Jose, Costa Rica. Remote sensing
184 observations from both the DC-8 and the ER-2 suggest that the peak convective outflow was
185 above the DC-8 ceiling, thus the in situ observations were in the lower part of the cirrus anvil.
186 On the 5 and 8 August flights the cirrus anvils extended westward from the convective cores
187 selected. On these flights the DC-8 was unable to reach cloud tops but was able to get near to the
188 top of the cirrus in later orbits. Seven complete orbits were flown on the 31 July flight and 5
189 complete orbits were flown on each of the 5 and 8 August flights (Figure 1). It should be noted
190 that during the 8 August flight the convective core feeding the initially selected cirrus anvil
191 dissipated, so the pattern was moved to fly in a newly formed anvil nearby. It should also be
192 noted that the DC-8 flew all of these orbits at the highest altitude safely obtainable limited by
193 aircraft weight. The altitude slowly increased as fuel was consumed and aircraft weight
194 decreased and can be seen figure 2. This provided an opportunity to sample each cloud at a range
195 of temperatures, decreasing from nearly 245 K for early passes to about 220 K for the later
196 passes for each flight.

During the cirrus cloud orbits on all three flights, HNO_3 generally oscillated between about 5 to nearly 75 pptv with the exception of large enhancements around t=55,500-56,500 seconds and t=59,000 seconds during the 31 July flight (Figures 2-4). The first large enhancement was observed on the 31 July flight when the aircraft briefly descended below the visible cloud base (discussed in section 4.3) and the second was during the turn at the far south eastern end of an orbit where the cirrus was thin and patchy (Figure 2, panel a). In general, the lowest HNO_3 mixing ratios of each orbit were observed at the upwind end of each orbit (closer to the cloud turret) and highest mixing ratios were at the downwind end. When orbits were repeated at constant altitude the variations of HNO_3 with respect to position were quite similar in successive passes over the established track. This is most clearly seen after t= 53,000 seconds on the 5 August flight (Figure 2, panel b). The trend in IWC was opposite in this orbit-scale pattern compared to HNO_3, being highest at the upwind end near the convective core (where HNO_3 was lowest) and decreasing downwind (Figure 2). Increases in IWC over shorter time intervals (smaller spatial scales) often coincided with decreased HNO_3 mixing ratios as well.

4. Discussion

4.1 General Observations

Mixing ratios of HNO_3 were significantly depressed in cirrus clouds sampled during TC4 compared to the mean mixing ratio of 120 pptv for all out of cloud measurements in the same 9 - 12 km upper tropospheric altitude range. Two processes may contribute to the lower mixing ratios. First, some fraction of the air inside the clouds may represent recent convectively pumped air in which HNO_3 could have been scavenged by precipitation in the updraft [e.g. Bertram et al., 2007], and second, cirrus ice crystals may have adsorbed HNO_3 in the UT surrounding the

convective outflow. The anticorrelation with IWC (Figure 2), sometimes observed over short time periods (e.g. Figure 2, panel c, ~t=49,000), suggests that the latter process plays an important role. Likewise, the sharp increase in HNO_3 mixing ratios observed during the dip below the visible cloud base at t=55,300 to t=56,500 (~9.5 km) on the 31 July flight (Figure 2, panel a and Figure 4) appears to reflect a release of HNO_3 from evaporating cirrus ice crystals. Such release suggests that there had to be considerable HNO_3 uptake by the cirrus ice. The fact that the DC-8 was often below the altitude of peak outflow in cirrus that had fallen out of the thickest part of the anvil would imply that a significant fraction of the sampled air surrounding the ice crystals had not been recently convected. Also, the observed increases of HNO_3 in thinner downwind regions of the study region have to reflect contributions of non-convected UT air because HNO_3 would not have been produced so quickly in detraining air depleted by scavenging [Bertram et al., 2007]. In a tracer study of this region, Avery et al. [this issue] conclude that the UT study region could represent an even mix of background long range transport pollution and air convected from ~2 – 3 km above the MBL, but not from the MBL directly. We assume that the observed depletions of HNO_3 are strongly influenced by uptake onto the cirrus crystals as the anvil detrained into UT air and/or the ice crystals settled into UT air below the altitude of maximum convective outflow.

4.2 Evidence for HNO_3 uptake onto cirrus ice particles

The premise that HNO_3 was depleted in cirrus clouds is based on comparisons to background observations made in cloud-free air at 9 - 12 km altitude during TC4. For quantification, a background needs to be defined. A mean mixing ratio of ~60 pptv was observed in UT clear air in the immediate vicinity of the racetracks during these three flights. This air, so close to strong convection, may contain a significant fraction of cloud processed air and

represent too low of a background estimate. While 60 pptv is higher than in-cloud observations (consistently < 40 pptv on the last 5 orbits of the 31 July flight and all orbits on the 5 and 8 August flights) it is indeed only half the mission mean (excluding transit flights to and from Costa Rica) of 120 pptv in the larger subtropical study region UT. Based on this, we assume background mixing ratios of HNO_3 in the UT near Costa Rica into which deep convection was detraining were likely in this range of 60 - 120 pptv. In the following it is assumed that 100 pptv is a reasonable estimate of UT HNO_3 before the cirrus formed. This is consistent with the value given by Kärcher and Voigt [2006] as an average over many other field campaigns and was subsequently used by Krämer et al. [2008] in their model of HNO_3 partitioning in cirrus clouds. In-cirrus HNO_3 was observed at 5 - 75% of this assumed background, most often in the range 10 - 40% (Figure 2). And, as noted earlier, the depressed mixing ratios in the anvils could be attributed to simple mixing of background UT air and recently convected air that had HNO_3 removed by scavenging. However, if we accept the convected fraction estimate from Avery et al. [this issue], this would still yield HNO_3 mixing ratios ~50 pptv in the lower parts of the anvils sampled by the DC-8. Alternatively, we postulate that uptake onto cirrus ice accounts for much of the observed depletion of HNO_3 and that at DC-8 flight levels. While contributions from mixing are not being ruled out, disregarding it provides constraint on the maximum uptake of HNO_3 onto the cirrus particles in the warm ITCZ clouds.

The inferred uptake onto cirrus ice is simply the 100 pptv background minus observed in-cloud HNO_3 mixing ratio. This value was calculated for each HNO_3 sample interval when IWC was detectable. The delta HNO_3 was converted to volumetric number density using in situ pressure and temperature and then divided by mean observed SAD over each integration interval. Surface coverages of 0.01 to .67 $x10^{14}$ molecules$\cdot cm^{-2}$ were estimated, with substantial scatter

(Figure 3, gray dots). To examine temperature dependence, we estimated average surface coverages in 5 degree K temperature bins ranging from ~219 K to ~243 K. Table 1 and Figure 3 (blue triangles) suggest two-fold more uptake at the coldest temperature compared to the warmest, but the trend is not smooth nor statistically significant. We note, however, that the estimated coverages during TC4 are quite similar to those reported by Zieris et al. [2004] for temperatures of ~227 K and substantially smaller than all previous observations at temperatures below 220 K except for the anomalously low coverages reported by Melinger et al. [1999] at 196 K. The TC4 surface coverage estimates are plotted with the temperature-bin-average HNO_3 molecular coverages from CRYSTAL-FACE reported by Popp et al. [2004] from ~198 K to ~218 K to show the full range of temperatures for which field observations have been reported (Figure 3). In addition, we used the non-dissociative Langmuir isotherm fit from the Ullerstam et al. [2005] laboratory experiments to predict surface molecular coverages at mean in situ temperatures for each TC4 sample,

$$\Theta = \Theta_{max} \times \frac{(K_{eq} P)^{v}}{1 + (K_{eq} P)^{v}}$$

where $v = 1$ (non-dissociative isotherm) and K_{eq} is the temperature dependant equilibrium constant from Ullerstam et al. [2005],

$$K_{eq} = -(5.1 \pm 0.4) \times 10^{5} T + (12.3 \pm 0.9) \times 10^{7}$$

assuming Θ_{max} = 2.4 x 10^{14} molecules·cm^{-2} as found in the thin film studies. We calculated predicted Θ during the racetrack anvil encounters using this empirical model, observations of gas phase HNO_3 partial pressure and temperature for each ~85 second measurement interval. We then calculated average Θ values for the same 5 discrete temperature bins between ~219 K and

~243K. Results are shown as red circles in figure 3. Predicted average Θ in these temperature bins are quite similar to the observations but show stronger temperature dependence than is apparent or even present in the observations. However, if measurements presented here are compared to measurements made at colder temperatures during CRYSTAL-FACE [Popp et al. 2004], a potential temperature dependence could be inferred (figure 3).

The Ullerstam et al. [2005] non-dissociative isotherm model appears to capture our estimates of HNO_3 uptake onto ices surface in the tropical cirrus anvils in the TC4 study regions of the intertropical convergence zone very well. This is a departure from many previous field studies where coverages predicted by isotherm models were often a factor of two or more higher than estimates based on the observations (noted by Ullerstam et al., 2005). Because the surface coverage estimates based on decreased HNO_3 neglecte mixing with scavenged air, the means in the 5 temperature bins have to be upper limits. However if the estimated coverages were reduced by half (on average) to account for dilution, the means would be even closer to those estimated by the isotherm model in 3 of the 5 temperature bins, and the one standard deviation error bars would still overlap in all of the bins. The very low HNO_3 vapor pressures and high SAD encountered in the TC4 study region may have led to a system more closely reflecting the equilibrium required for the isotherm model to be applicable. Reported HNO_3 vapor pressures in the study region of most prior field campaigns were typically much higher than observed here.

On the other hand, even though the two estimates of surface coverage in the TC4 clouds agree statistically, our estimates based on the apparent loss of gas phase HNO_3 show little or no dependence on temperature, while coverages estimated from the isotherm model markedly decrease above 225 K. It should also be noted that there is considerably more scatter in estimates based on measured HNO_3 and SAD than those based on measured HNO_3 and K in each

of the temperature bins (Figure 3), reflecting the key role of available surface area. Ullerstam et al. [2005] pointed out that the fact that cirrus crystals are rarely stable in size (constantly growing or shrinking in response to the local water vapor field) was a likely contributor to the disagreement between laboratory-based models and real clouds. Likewise, Popp et al. [2004] suggested that shortcomings of equilibrium model approaches can be explained, in part, by significant variations in HNO_3 mixing ratios in and around cirrus. In particular, settling of ice crystals will generally quickly remove them from any region where they may have been near to equilibrium. Evidence of such particle settling (and release of HNO_3 that had been adsorbed at higher altitude) during TC4 is presented in section 4.3. It appears that the agreement between our estimates of surface coverage and estimates based on the isotherm model was more likely fortuitous, than an indication that the TC4 tropical cirrus anvils were generally closer to equilibrium than clouds sampled in previous experiments. The extensive sampling time spent in these clouds allowed averaging over a large number of airmasses that were each likely not truly in equilibrium, but to differing degrees.

The estimated surface coverages of HNO_3 on cirrus ice during TC4 represent fractional coverages up to 28% of a molecular monolayer (Θ) for an extreme case (based on 2.4×10^{14} molecule$\cdot$cm^{-2} from Ullerstam et al., [2005]), with the bin means (Table 1) only ranging from 3 to 5 %. Clearly, uptake does not result in monolayer coverages in these warm clouds, especially considering that our estimates are based on the assumption that all of the observed depletion of is attributed to uptake by ice. Conversely, the depression of HNO_3 mixing ratios in the cirrus was substantial (on the order of 60 - 90%) and might have implications for chemistry in the UT if the removal was irreversible. However, the dip below cloud base discussed in section 4.3 during the

329 31 July flight suggests that vertical redistribution of HNO_3 by sedimenting cirrus ice may involve
330 only modest displacements.

331 4.3 Vertical Redistribution of Nitric Acid by Cirrus

332 Sedimentation of cirrus ice crystals with adsorbed HNO_3 has been postulated as an
333 efficient mechanism to remove HNO_3 from the UT [Lawrence and Crutzen, 1998]. Tropical
334 cirrus have been suggested to have the highest potential to vertically redistribute HNO_3 [Krämer
335 et al., 2008]. This occurs when cirrus ice particles grow large enough for gravitational settling to
336 remove them from the cirrus cloud. As ice particles settle out of the cloud into much dryer air
337 below, sublimation releases adsorbed HNO_3 taken up in the cloud into the below cloud air. A
338 key question is how far downward the particles carry the HNO_3 before release. As noted earlier,
339 about halfway through the series of orbits during the 31 July flight the DC-8 slowly descended to
340 the cloud base (Figure 2, panel a). Figure 4 is a detailed view of the time period during the
341 descent below the cloud base. It can been seen that while skimming the cloud base, HNO_3 was
342 observed to be enhanced by more than 120 pptv compared to the 20 pptv observed in thick cloud
343 immediately preceding descent. After several minutes of level flight, the aircraft descended an
344 additional 500 meters further below the cloud where HNO_3 decreased to about 60 pptv. The
345 aircraft then began a slow ascent and the thin layer of enhanced HNO_3 was again observed at the
346 cloud base. Vertical profiles of both ascent and descent are presented in Figure 5. These data are
347 consistent with the hypothesized redistribution of HNO_3 by cirrus cloud particle sedimentation
348 and subsequent evaporation as described in depth by Lawrence and Crutzen [1998], however, the
349 layer of enhancement observed here is remarkably thin and extremely close to the cloud base
350 Presumably, larger ice crystals like those observed in CRYSTAL-FACE might carry HNO_3

351 further below cloud base (Popp et al., 2004) but vertical redistribution by the cirrus clouds
352 sampled from the DC-8 in TC4 appears limited to the thickness of the cirrus anvil.

353 5. Conclusions

354 HNO_3, IWC, and SAD observations in warm cirrus anvils (~219K-243K) during three
355 focused and repeated encounters in the tropical UT near Costa Rica during the NASA TC4 field
356 campaign in 2007 are presented. In-cloud depletions of gas-phase HNO_3 were observed and were
357 positively correlated to increasing cloud water content and ice surface area. Based on
358 observations from the same study, we assume that the out-of-cloud HNO_3 background mixing
359 ratio is approximately 100 pptv and the difference in observations made while in-cloud represent
360 HNO_3 adsorbed onto ice particles. With these assumptions, average molecular coverages of
361 HNO_3 on ice particles ranged from 0.7 x 10^{13} to 1.3 x 10^{13} molecules·cm^{-2} for 5 different
362 temperature bins. Our observations suggest that uptake was not limited by available ice surfaces
363 as these coverages represent about 3 to 5% of a monolayer (assuming Θ_{max} = 2.4x10^{14}
364 molecules·cm^{-2}). However, this was enough to affect up to about a 90% depletion of HNO_3 at
365 periods of high IWC and SAD. Although there is no obvious temperature dependence seen in our
366 molecular surface coverage on ice, our observations appear to be slightly less than those
367 presented in Popp et al. [2004] from measurements made during CRYSTAL-FACE in slightly
368 cooler tropical upper tropospheric cirrus cloud. This supports prior laboratory work suggesting a
369 negative temperature dependence on uptake. Evidence of gravitational settling and subsequent
370 evaporation of cirrus ice particles releasing HNO_3 back to the gas phase was observed during the
371 31 July flight, however the magnitude of this single event is not sufficient to support large scale
372 redistribution of HNO_3 similar to that described by Lawrence and Crutzen [1998]. Further
373 investigations into the magnitude of the redistributive capabilities of cirrus clouds would benefit

374 from repeated vertical profiles in and beneath such formations and would ideally include direct

375 in situ measurements of both gas and condensed-phase HNO_3.

376 Acknowledgements

377 TC4 was sponsored by the NASA Headquarters Atmospheric Composition Focus Group which
378 includes the Tropospheric Chemistry Program, Upper Atmospheric Research Program and
379 Radiation Science Program.

380 References.

381 Abbatt, J. P. D. (1997), Interaction of HNO_3 with water-ice surfaces at temperatures of the free
382 troposphere, *Geophys. Res. Lett.*, *24*(12), 1479-1482.
383
384 Arora, O. P., D. J. Cziczo, A. M Morgan, J. P. D. Abbott, R. F. Niedziela (1999), Uptake of nitric acid by
385 sub-micron-sized ice particles, *Geophys. Res. Lett.*, *26*(24), 3621-3624.
386
387 Avery, M., J. Joiner, C. Twohy, E, Atlas, D. Blake, P. Bui, J. Crounse, G. Diskin, P. Lawson, D. McCabe,
388 M. McGill, P. Pilewski, D. Rogers, G. Sachse, R. Salawitch, S. Schmidt, K. Severance, A. Thompson, C.
389 Trepte,and P. Wennberg (this issue), Convective Distribution of Tropospheric Ozone and Tracers in the
390 Central American ITCZ Region: Evidence from Observations During TC4, submitted to *J. Geophys. Res.*
391
392 Bertram, T. H., et al. (2007), Direct measurements of the convective recycling of the upper troposphere,
393 *Science*, 315(5813), 816-820, doi: 10.1126/science.1134548.
394
395 Field, P. R., A. J. Heymsfield, and A. Bansemer (2006) Shattering and particle interarival times measured
396 by optical array probes in ice clouds. *J. Atmos. Ocean. Tech.*, 23, 1357--1371.
397
398 Hinds, W.C. Acceleration and curvilinear particle motion, *Aerosol Technology*, pp.
399 105-110, John Wiley & Sons, Inc., New York, 1982.

400
401
402
403
404

405 Hudman, R. C., D. J. Jacob, S. Turquety, E. M. Leibensperger, L. T. Murray, S. Wu, A. B. Gilliland, M.
406 Avery, T. H. Bertram, W. Brune, R. C. Cohen, J. E. Dibb, F. M. Flocke, A. Fried, J. Holloway, J. A.
407 Neuman, R. Orville, A. Perring, X. Ren, G. W. Sachse, H. B. Singh, A. Swanson, P. J. Wooldridge(2007),
408 Surface and lightning sources of nitrogen oxides over the United States: magnitudes, chemical evolution,
409 and outflow, *J. Geophys. Res*., *112*, D12S05, doi:10.1029/2006JD007912
410
411 Hudson, P. K., J.E. Shilling, M. A. Tolbert, O. B. Toon (2002), Uptake of nitric acid on ice at
412 tropospheric temperatures: Implications for cirrus clouds, *J. Phys. Chem. A*, *106*, 9874-9882.
413
414 Hynes, R. G. M. A. Fernandez, R. A. Cox (2002), Uptake of HNO_3 on water-ice and coadsorption of
415 HNO_3 and HCl in the temperature range 210-235 K, *J. Geophys. Res.*, *107*(D24), 11,
416 doi:10.1029/2001JD001557.
417
418 Jacob, D. J., et al. (1996), Origin of ozone and NO_x in the tropical troposphere: A photochemical analysis
419 of aircraft observations over the South Atlantic basin, *J. Geophys. Res.*, *101*(D19), 24235-24250.
420
421 Jensen, E. J., Lawson, P., Baker, B., Pilson, B., Mo, Q., Heymsfield, A. J., Bansemer, A., Bui, T.P.,
422 McGill, M., Hlavka, D., Heymsfield, G., Platnick, S., Arnold, G. T., and Tanelli, S. (2009), On the
423 importance of small ice crystals in tropical anvil cirrus, *Atmos. Chem. Phys. Discuss.*, *9*, 5321-5370.
424
425 Kärcher, B., and C. Voigt (2006), Formation of nitric acid/water ice particles in cirrus clouds, *Geophys.*
426 *Res. Lett*., 33, L08806, doi:10.1029/2006GL025927.
427
428 Krämer, M., Schiller, C., Voigt, C., Schlager, H., Popp, P.J. (2008), A climatological view of HNO3
429 partitioning in cirrus clouds, Q. J. R. Meteorol. Soc., doi:10.1002/qj.253.
430

Kondo, Y., et al. (2003), Uptake of reactive nitrogen on cirrus cloud particles in the upper troposphere and lowermost stratosphere, *Geophys. Res. Lett.*, *30*(4), 1154, doi:10.1029/2002GL015549.

Lawrence, M. G., and P. J. Crutzen (1998), The impact of cloud particle gravitational settling on soluble trace gas distributions, *Tellus Ser.B, 50*, 263-289.

Meier, A., and J. Hendricks (2002), Model studies on the sensitivity of upper tropospheric chemistry to heterogeneous uptake of HNO_3 on cirrus ice particles, *J. Geophys. Res.*, *107*(D23), 4696, doi:10.1029/2001JD000735.

Meilinger, S. K., et al. (1999), HNO_3 partitioning in cirrus clouds, *Geophys. Res. Lett.*, *26*(14), 2207-2210.

Neuman, J. A., et al. (2001), In situ measurements of HNO_3, NO_y, NO, and O_3 in the lower stratosphere and upper troposphere, *Atmos. Environ*, *35*(33), 5789-5797.

Pierce, R. B., et al. (2007), Chemical data assimilation estimates of continental U.S. ozone and nitrogen budgets during the Intercontinental Chemical Transport Experiment–North America, *J. Geophys. Res.*, 112, D12S21, doi:10.1029/2006JD007722.

Popp, P. J., et al. (2004), Nitric acid uptake on subtropical cirrus cloud particles, *J. Geophys. Res.*, *109*, D06302, doi:10.1029/2003JD004255.

Staudt, A. C., D. J. Jacob, F. Ravetta, J. A. Logan, D. Bachiochi, T. N. Krishnamurti, S. Sandholm, B. Ridley, H. B. Singh, B. Talbot (2003), Sources and chemistry of nitrogen oxides over the tropical Pacific, *J. Geophys. Res.*, *108*(D2), 8239, doi10.1029/2002JD002139.

457 Tabazadeh, A., O. B. Toon, E. J. Jensen, (1999), A surface chemistry model for nonreactive trace gas
458 adsorption on ice: Implications for nitric acid scavenging by cirrus, *Geophys. Res. Lett.*, *26*(14), 2211-
459 2214.
460
461 Thakur, A. N., H. B. Singh, P. Mariani, Y. Chen, Y. Wang, D. J. Jacob, G. Brasseur, J. F. Muller, M.
462 Lawrence (1999), Distribution of reactive nitrogen species in the remote free troposphere: data and model
463 comparisons, *Atmos. Environ.*, *33*(9), 1403-1422.
464
465 Tian, L., G. M. Heymsfield, A. J. Heymsfield, A. Bansemer, L. Li, C. H. Twohy, and R. C. Srivastava,
466 (2009), A study of cirrus ice particle size distribution using TC4 observations, *Submitted to J. Atmos. Sci.*
467
468 Toon, O. B., D. O. Starr, E. J. Jensen, P. A. Newman, S. E. Platnick, M. R. Schoeberl, P. O. Wennberg, S.
469 C. Wofsy, M. J. Kurylo, H. Maring, K. W. Jucks, M. S. Craig, M. F. Vasquez, L. Pfister, K. Rosenlof, H.
470 B. Selkirk, P. R. Colarco, S. R. Kawa, G. G. Mace, P. Minnis, K. E. Pickering (this issue), Planning and
471 implementation of the Tropical Composition, Cloud, and Climate Coupling Experiment (TC4), submitted
472 to *J. Geophys. Res.*
473
474 Twohy, C. H., A. J. Schanot, W. A. Cooper (1997), Measurement of condensed water content in liquid
475 and ice clouds using an airborne counterflow virtual impactor, *J. Atmos. Oceanic Technol.*, *14*(1), 197-
476 202.
477
478 Ullerstam, M. T. Thornberry, J. P. D. Abbatt (2005), Uptake of gas-phase nitric acid to ice at low partial
479 pressures: evidence for unsaturated surface coverage, *Faraday Discuss*, *130*, 211-226.
480
481
482

Weinheimer, A. J., T. L. Campos, J. G. Walega, F. E. Grahek, B. A. Ridley, D. Baumgardner, C. H. Twohy, B. Gandrud, E. J. Jensen (1998), Uptake of NO_y on wave-cloud ice particles, *Geophys. Res. Lett.*, *25*(10), 1725-1728.

Ziereis, H., et al. (2004), Uptake of reactive nitrogen on cirrus cloud particles during INCA, *Geophys. Res. Lett.*, *31*, L05115, doi:10.1029/2003GL018794.

Zondlo, M. A. S. B. Barone, M. A. Tolbert (1997), Uptake of HNO_3 on ice under upper tropospheric conditions, *Geophys. Res. Lett.*, *24*(11), 1391-1394.

492 Figure 1. Map of racetrack maneuvers during TC4 flights on 31 July and 5 and 8 August. Circles
493 represent measurements of condensed water content in $g \cdot m^{-3}$ averaged to the HNO_3 measurement
494 integration time and show progression of aircraft in and out of heavy cirrus cloud.
495
496 Figure 2. Time series measurements made during the racetrack maneuvers of gas phase HNO_3
497 mixing ratios (solid black) and condensed water content (solid gray) averaged to HNO_3
498 instrument integration time on the 31 July flight (a), the 5 August flight (b) and the 8 August
499 flight (c) respectively. IWC data on the 31 July flight has discontinuities relative to HNO_3 that
500 are ignored for plotting. Pressure altitude (dashed gray) and longitude (solid thin) are shown for
501 spatial reference.
502
503 Figure 3. HNO_3 molecular coverage versus temperature. Solid gray circles represent discrete
504 values calculated while in cirrus cloud during TC4 flights on 31 July and 5 and 8 August using
505 SAD averaged to HNO_3 integration periods, measured HNO_3 mixing rations and an assumed
506 cirrus-free 100 pptv background HNO_3 mixing ratio. Blue triangles represent average TC4
507 coverages for 5° temperature bins ~219 K to ~243 K. Green squares represent average coverages
508 from Popp et al. [2004] figure 10 calculated for SADs greater than 200 $\mu m^2 \cdot cm^{-3}$ from data
509 obtained during the CRYSTAL-FACE campaign. Error bars represent one standard deviation of
510 the mean in each temperature bin. Open red circles represent mean predicted molecular
511 coverages predicted using the Langmuir isotherm model presented in Ullerstam et al. [2005] and
512 discrete TC4 P_{HNO3} and temperature measurements from each ~85 second long sample interval.
513
514

Figure 4. Time series plot from t=54000 seconds to t=57000 seconds on the 31 July flight showing enhanced layer of gas phase HNO_3 just below the visible cloud base. HNO_3 mixing ratios decreased by a factor of 2 during the subsequent descent to ~0.5 km below the cloud base. The enhanced layer was also sampled during ascent back into the clouds.

Figure 5. Vertical profile of gas phase HNO_3 from the 31 July flight from t=54800 seconds to t=56000 seconds. The enhanced layer can be clearly seen during both descent and ascent just below 9.5km, immediately below the visible base of the cirrus anvil.

523 Table 1. Mean in-cloud ice surface area density and estimated mean HNO_3 molecular coverage

524 during racetrack maneuvers from TC4 flights on 31 July and 5 and 8 August.

525

Temperature Bin	Mean Temperature K (Std.Dev.) *(range)*	Molec · cm^{-2} Surface Area x 10^{13} (Std.Dev) (*range*)	Ice Surface Area (SAD) $\mu m^2 \cdot cm^{-3}$ (Std.Dev.) *(range)*
219-224	223.1 (1.2) *(219.6-224.0)*	1.3 (0.9) *(0.3-4.2)*	3507 (2558) *(712-10677)*
224-229	225.5 (1.3) *(224.0-228.9)*	0.9 (0.5) *(0.3-2.5)*	3673 (2190) *785-10701*
229-234	230.1 (1.2) *(229.0-233.4)*	0.9 (0.8) *(0.1-3.7)*	6600 (6562) *412-32256*
234-239	235.8 (1.3) *(234.3-238.9)*	1.0 (1.2) *(0.1-6.7)*	6591 (5414) *415-23418*
239+	240.7 (1.1) *(239.3-242.8)*	0.7 (0.6) *(0.1-2.3)*	7267 (7998) *56-38344*

526

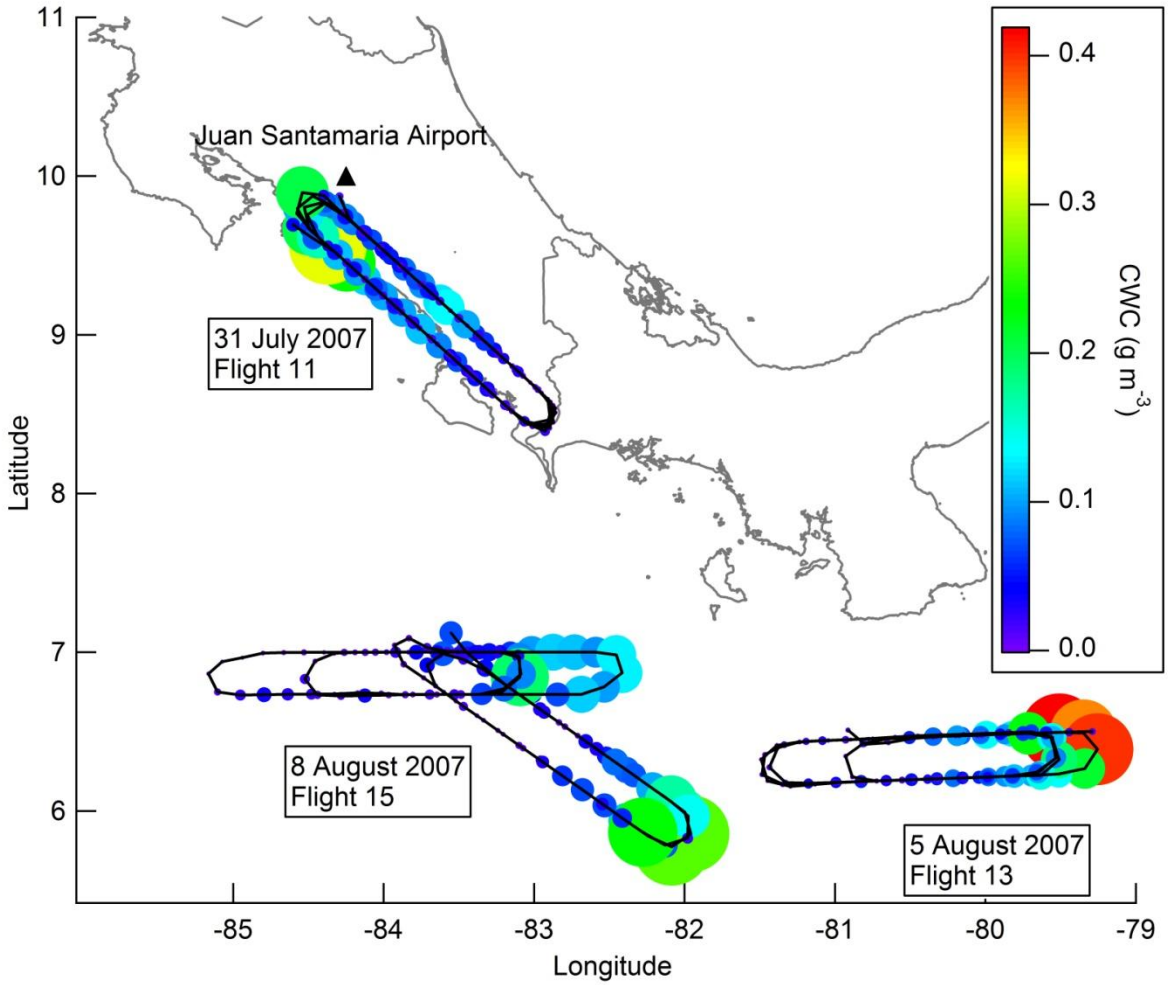

527

528 Figure 1. Map of racetrack maneuvers during TC4 flights on 31 July and 5 and 8 August. Circles
529 represent measurements of condensed water content in $g \cdot m^{-3}$ averaged to the HNO_3 measurement
530 integration time and show progression of aircraft in and out of heavy cirrus cloud.

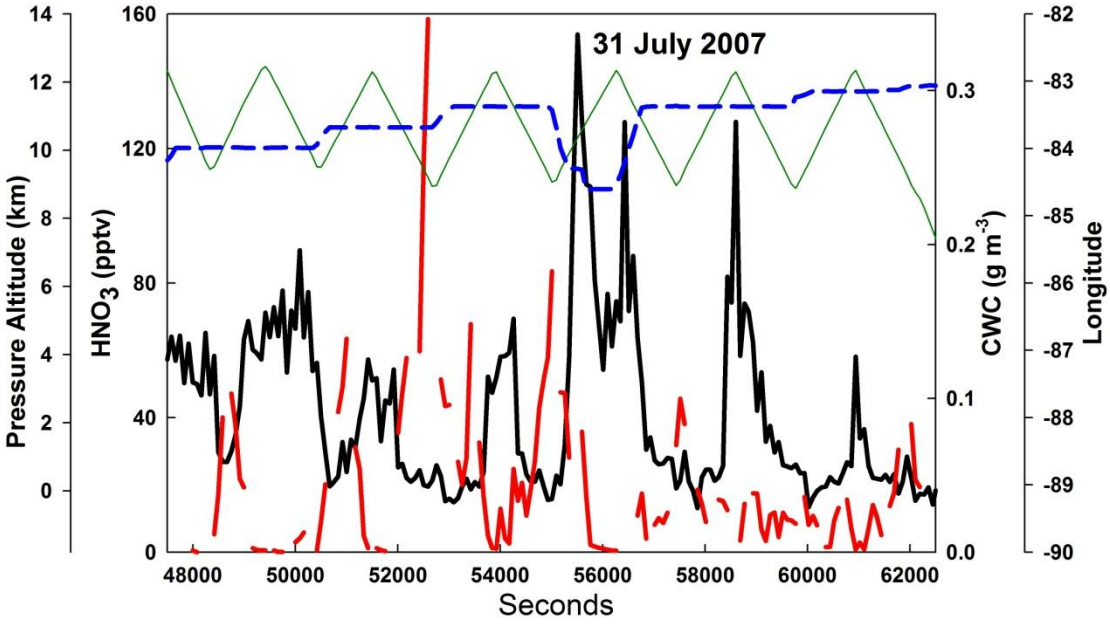

531

532 Figure 2(a).

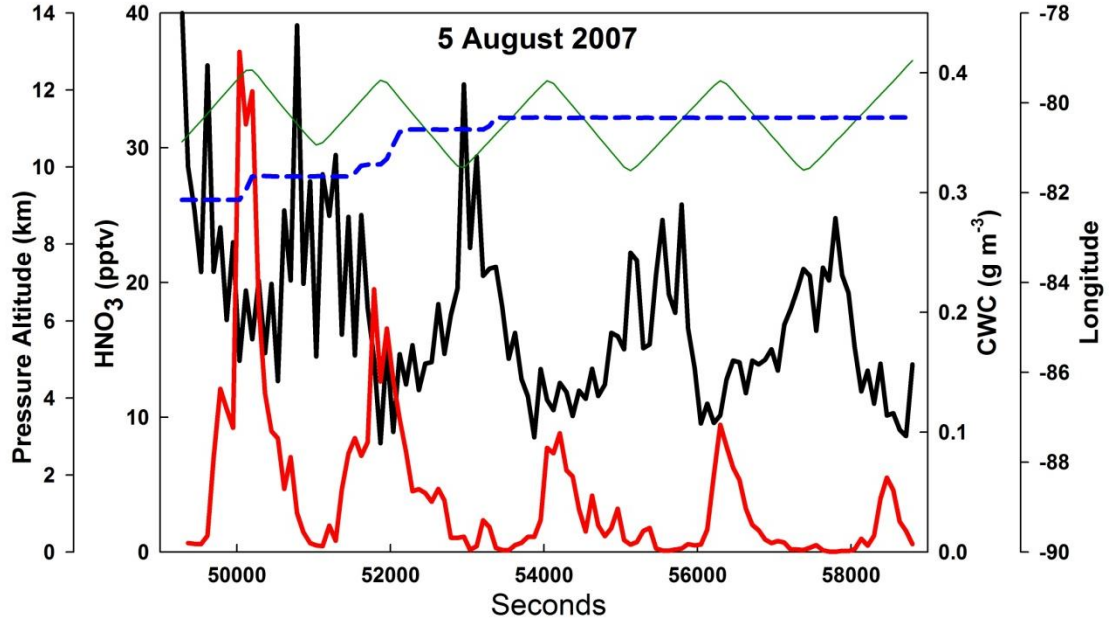

533

534 Figure 2(b).

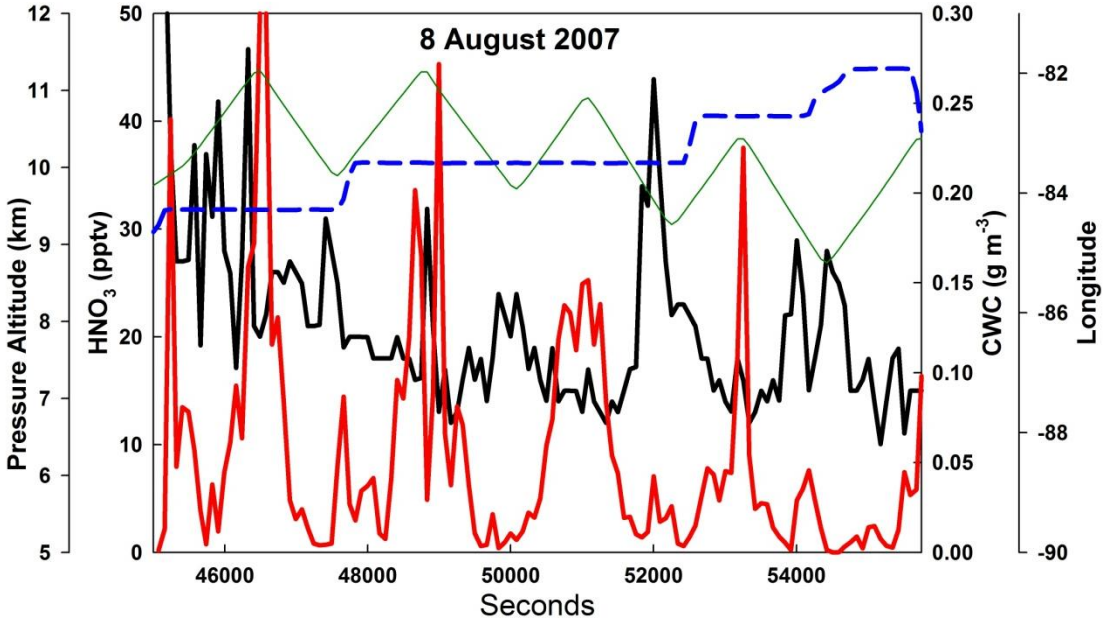

535

536 Figure 2(c).

537 Figure 2. Time series measurements made during the racetrack maneuvers of gas phase HNO_3
538 mixing ratios (solid black) and condensed water content (red) averaged to HNO_3 instrument
539 integration time on the 31 July flight (a), the 5 August flight (b) and the 8 August flight (c)
540 respectively. IWC data on the 31 July flight has discontinuities relative to HNO_3 that are ignored
541 for plotting. Pressure altitude (dashed blue) and longitude (solid green) are shown for spatial
542 reference.

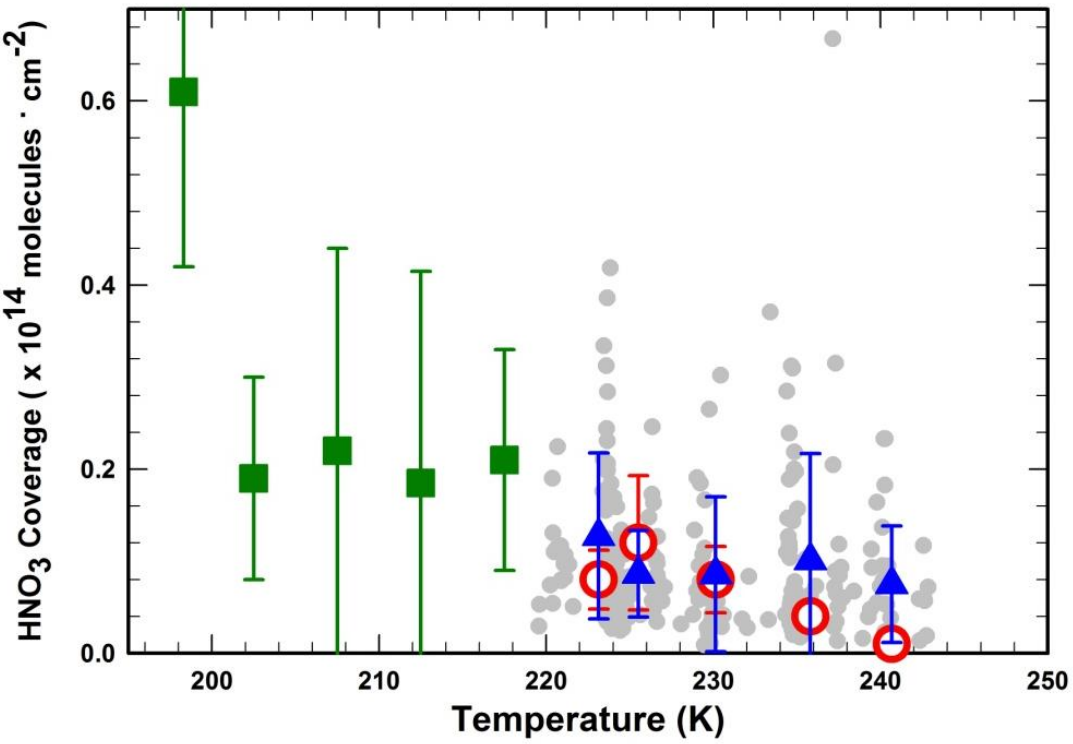

Figure 3. HNO_3 molecular coverage versus temperature. Solid gray circles represent discrete values calculated while in cirrus cloud during TC4 flights on 31 July and 5 and 8 August using SAD averaged to HNO_3 integration periods, measured HNO_3 mixing rations and an assumed cirrus-free 100 pptv background HNO_3 mixing ratio. Blue triangles represent average TC4 coverages for 5° temperature bins ~219 K to ~243 K. Green squares represent average coverages from Popp et al. [2004] figure 10 calculated for SADs greater than 200 $\mu m^2 \cdot cm^{-3}$ from data obtained during the CRYSTAL-FACE campaign. Error bars represent one standard deviation of the mean in each temperature bin. Open red circles represent mean predicted molecular coverages predicted using the Langmuir isotherm model presented in Ullerstam et al. [2005] and discrete TC4 P_{HNO3} and temperature measurements from each ~85 second long sample interval.

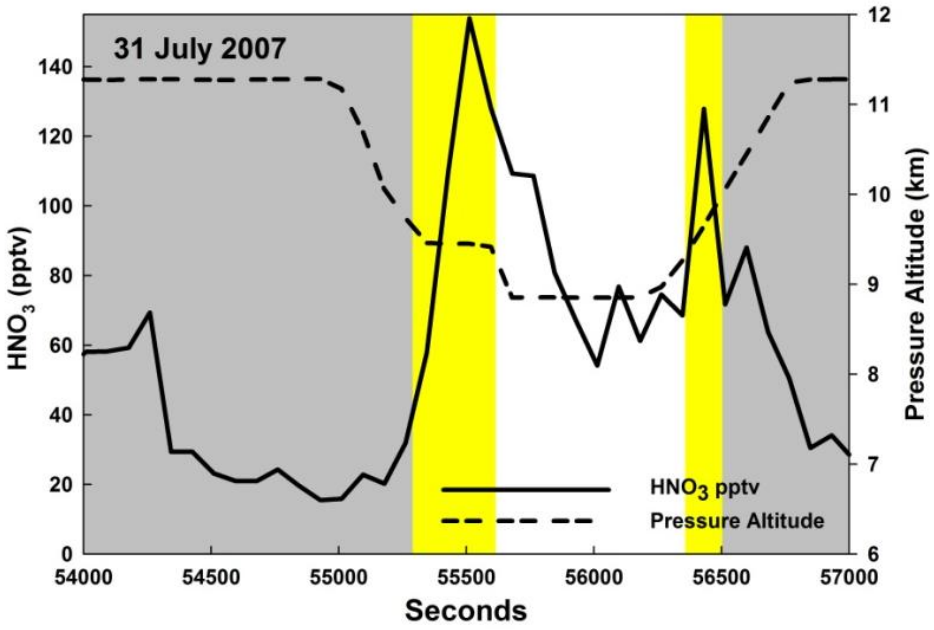

554

555 Figure 4. Time series plot from t=54000 seconds to t=57000 seconds on 31 the July flight
556 showing enhanced layer of gas phase HNO_3 just below the visible cloud base (shaded yellow
557 region). HNO_3 mixing ratios decreased by a factor of 2 during the subsequent descent to ~0.5 km
558 below the cloud base (unshaded region). The enhanced layer was also sampled during ascent
559 back into the clouds (gray shaded region).

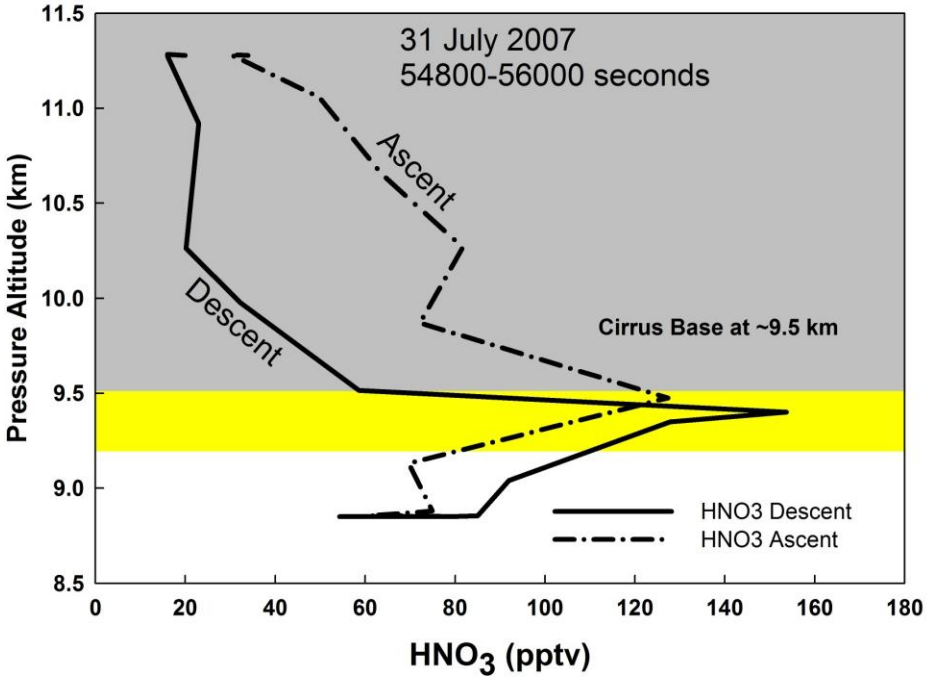

560

561 Figure 5. Vertical profile of gas phase HNO_3 from the 31 July flight from t=54800 seconds to
562 t=56000 seconds. The enhanced layer can be clearly seen during both descent and ascent just
563 below 9.5km, immediately below the visible base of the cirrus anvil.